Iron-Blocking the High-Affinity Mn-Binding Site in Photosystem II Facilitates Identification of the Type of Hydrogen Bond Participating in Proton-Coupled Electron Transport via $Y_Z^{\bullet}$†

Boris K. Semin,[#,‡] Elena R. Lovyagina,[‡] Kirill N. Timofeev,[‡] Ilya I. Ivanov,[‡] Andrei B. Rubin,[‡] and Michael Seibert*[,#]

Basic Sciences Center, National Renewable Energy Laboratory, Golden, Colorado 80401, and Department of Biophysics, Faculty of Biology, Moscow State University, Moscow 119899, Russian Federation

Received November 10, 2004; Revised Manuscript Received May 17, 2005

ABSTRACT: Incubation of Mn-depleted PSII membranes [PSII(−Mn)] with Fe(II) is accompanied by the blocking of $Y_Z^{\bullet}$ at the high-affinity Mn-binding site to exogenous electron donors [Semin et al. (2002) *Biochemistry 41*, 5854−5864] and a shift of the pK_{app} of the hydrogen bond partner for Y_Z (base B) from 7.1 to 6.1 [Semin, B. K., and Seibert, M. (2004) *Biochemistry 43*, 6772−6782]. Here we calculate activation energies (E_a) for $Y_Z^{\bullet}$ reduction in PSII(−Mn) and Fe-blocked PSII(−Mn) samples [PSII(−Mn, +Fe)] from temperature dependencies of the rate constants of the fast and slow components of the flash-probe fluorescence decay kinetics. At pH < pK_{app} (e.g., 5.5), the decays are fit with one (fast) component in both types of samples, and E_a is equal to 42.2 ± 2.9 kJ/mol in PSII(−Mn) and 46.4 ± 3.3 kJ/mol in PSII(−Mn, +Fe) membranes. At pH > pK_{app}, the decay kinetics exhibit an additional slow component in PSII(−Mn, +Fe) membranes (E_a = 36.1 ± 7.5 kJ/mol), which is much lower than the E_a of the corresponding component observed for $Y_Z^{\bullet}$ reduction in PSII(−Mn) samples (48.1 ± 1.7 kJ/mol). We suggest that the above difference results from the formation of a strong low barrier hydrogen bond (LBHB) between Y_Z and base B in PSII(−Mn, +Fe) samples. To confirm this, Fe-blocking was performed in D_2O to insert D^+, which has an energetic barrier distinct from H^+, into the LBHB. Measurement of the pH effects on the rates of $Y_Z^{\bullet}$ reduction in PSII(−Mn, +Fe) samples blocked in D_2O shows a shift of the pK_{app} from 6.1 to 7.6, and an increase in the E_a of the slow component. This approach was also used to measure the stability of the $Y_Z^{\bullet}$ EPR signal at various temperatures in both kinds of membranes. In PSII(−Mn) membranes, the freeze-trapped $Y_Z^{\bullet}$ radical is stable below 190 K, but half of the $Y_Z^{\bullet}$ EPR signal disappears after a 1-min incubation when the sample is warmed to 253 K. In PSII(−Mn, +Fe) samples, the trapped $Y_Z^{\bullet}$ radical is unstable at a much lower temperature (77 K). However, the insertion of D^+ into the hydrogen bond between Y_Z and base B during the blocking process increases the temperature stability of the $Y_Z^{\bullet}$ EPR signal at 77 K. Again, these results indicate that Fe-blocking involves Y_Z in the formation of a LBHB, which in turn is consistent with the suggested existence of a LBHB between Y_Z and base B in intact PSII membranes [Zhang, C., and Styring, S. (2003) *Biochemistry 42*, 8066−8076].

The oxidized primary donor, $P680^+$, in photosystem II (PSII)[1] reaction centers, formed during the initial steps of the charge-separation process, is rapidly re-reduced by the redox-active tyrosine secondary donor, Y_Z, located at position 161 on the D1 polypeptide in plants. In the reduced form, Y_Z may exist as a tyrosinate anion (Y_Z^-) or a neutral tyrosine (Y_Z) depending on the pH (*1*). The protonation state of reduced Y_Z in O_2-evolving preparations of PSII has been studied using both optical (*2*, *3*) and FTIR (*4*) spectroscopies. The optical difference spectra reported by Candeias et al. (*2*) and Haumann et al. (*3*) imply that Y_Z is a tyrosinate in intact PSII at physiological pH (see also ref *5* for a discussion). However, Noguchi et al. (*4*), based on FTIR measurements using O_2-evolving PSII core complexes from *Synechocystis* 6803 at pH 6.0, suggested that Y_Z is protonated. The protonation state of oxidized Y_Z in O_2-evolving preparations of PSII has not been studied rigorously because of the very short lifetime of the tyrosine radical. However,

† This work was sponsored in part by the Division of Energy Biosciences, Office of Science, U.S. Department of Energy (MS) and by the Russian Foundation for Basic Research (ABR).

* To whom correspondence should be addressed. Telephone: (303) 384-6279. Fax: (303) 384-6150. E-mail: mike_seibert@nrel.gov.

[#] National Renewable Energy Laboratory.

[‡] Moscow State University.

[1] Abbreviations: Chl, chlorophyll; DCMU, 3-(3,4-dichlorophenyl)-1,1-dimethylurea; DPC, 1,5-diphenylcarbazide; F_0, fluorescence emitted by a sample at low light levels prior to flash excitation; $(F - F_0)/F_0$, fluorescence yield; E_a, activation energy; HA_Z, high-affinity electron donation site to $Y_Z^{\bullet}$ by Mn(II); MES, 2-(*N*-morpholino) ethanesulfonic acid; LBHB, low barrier hydrogen bond; OEC, oxygen-evolving complex; P680, primary electron donor in PSII; pK_{app}, apparent p*K*; PSII, photosystem II; PSII(−Mn), Mn-depleted PSII membranes; PSII(−Mn, +Fe), Fe-blocked PSII(−Mn); Q_a, primary quinone acceptor of PSII; Q_b, secondary quinone acceptor of PSII; RC, reaction center; Tris, tris(hydroxymethyl)-aminomethane; Y_D, redox-active tyrosine D2-Tyr161, an alternative electron donor to $P680^+$ in PSII; Y_Z, redox-active tyrosine D1-Tyr161, the first electron donor to $P680^+$ in PSII; λ, reorganization energy.

10.1021/bi047618w CCC: $30.25
Published on Web 06/18/2005

from the isotropic g value for the Y_Z tyrosyl radical [$g = 2.004$ (*6*)], the spectrum has been assigned to the neutral (deprotonated) form of the tyrosine radical (*7*) and not to the cation radical [$g = 2.0033$ (*8*)].

The properties of the reduced and especially the oxidized forms of Y_Z have been examined more thoroughly in Mn-depleted PSII [PSII(−Mn)] preparations. FTIR measurements at pH 6.0 showed that the reduced form of Y_Z in PSII(−Mn) core complexes of *Synechocystis* sp. PCC 6803 WT is protonated (*9*). Diner et al. (*10*), using optical spectroscopy, also found that Y_Z is mostly protonated at neutral pH [apparent pK_a (pK_{app}) around 8.0−8.3]. Information about $Y_Z^\bullet$ in PSII(−Mn) preparations from ESE-ENDOR, cw ENDOR, and ESEEM measurements (*11*−*13*) as well as the g value measured for the tyrosyl radical (*6*) also indicate that it is a neutral radical.

The results above imply that the oxidation of tyrosine must be accompanied by the deprotonation of Y_Z. It is widely accepted that deprotonation of Y_Z during oxidation occurs via a hydrogen bond between Y_Z and a nearby group X (*14*) [or base B (*15*); for reviews see refs *1*, *5*, *16*, *17*]. Spectroscopic studies (*12*, *18*) and numerous kinetic investigations of the rate of electron transfer from Y_Z to $P680^+$ in the forward direction (*10*, *15*, *19*, *20*) or from P680 to $Y_Z^\bullet$ in the back reaction (*21*−*23*) reveal that $Y_Z^\bullet$ is hydrogen-bonded in PSII(−Mn) preparations. Recent studies indicate the involvement of only a single proton during the rate-limiting step of the Y_Z oxidation (*24*) or $Y_Z^\bullet Q_a^-$ recombination (*23*) processes. Kinetic results clearly demonstrate coupling between electron transfer and the deprotonation/protonation of $Y_Z/Y_Z^\bullet$. The rate of Y_Z oxidation increases with pH from tens of microseconds at acidic pH to microseconds or submicroseconds at alkaline pHs [p$K_{app} \approx$ 7 (*5*), 6.9−7.5 (*19*), 8.3 (*10*)], whereas the rate of $Y_Z^\bullet$ reduction in the recombination reaction decreases with pH from 10 ms to about 200 ms [pK_{app} value of 6.0 (*21*), 7.5 (*22*), 7.1 (*23*)]. The nature of the protonated group controlling the kinetics of Y_Z oxidation and recombination has been studied extensively. Its pK_{app} [7.1−7.5 as proposed by Ahlbrink et al. (Scheme 1A) (*15*), Mamedov et al. (*22*) and Semin and Seibert (*23*)] reflects the pK of the proton acceptor, base B. On the other hand, Diner et al. (*10*) and Ahlbrink et al. (Scheme 1B) (*15*) assigned the pK_{app} to the pK of Y_Z. Site-directed mutagenesis (*19*, *22*, *25*, *26*) and chemical substitution (*27*) studies have suggested that the hydrogen-bonded partner of Y_Z (X or B) is D1-His190.

The above studies with PSII(−Mn) preparations have been used to explain one of the main differences between intact and PSII(−Mn) membranes, namely, that the oxidation of Y_Z in apo-PSII occurs on the microsecond time scale, whereas in intact PSII material the most rapid oxidation phase is 3 orders of magnitude faster (*1*, *5*, *16*, *17*). On the basis of the structural coupling between the Mn cluster and Y_Z, shown using FTIR (*4*) and EPR (*28*) methods, some investigators think that Mn-depletion alters the interaction between Y_Z and the proton-acceptor, base B, so that the oxidation of Y_Z becomes rate-limited. Tommos and Babcock (*17*) explained the slow Y_Z oxidation rate in Mn-depleted preparations in terms of an increase in the reorganization energy (λ) of the apo-PSII relative to O_2-evolving materials. This in turn was thought to be due to an increase in water accessibility to the Y_Z site and a perturbation of the hydrogen-bonding geometry around the Y_Z/base B site following Mn depletion. The change in geometry may shift the pK of base B to alkaline pH (*15*) or disrupt the permanent hydrogen bond between Y_Z and its proton acceptor (*19*).

Another difference in the properties of Y_Z in intact PSII and PSII(−Mn) membranes is reflected in the temperature dependence of the Y_Z oxidation and $Y_Z^\bullet$ reduction processes. In PSII(−Mn) membranes Y_Z oxidation does not occur below 180 K (*24*), but $Y_Z^\bullet$ can be trapped at temperatures between 240 and 273 K (*29*, *30*) by freezing the sample during illumination. However, the trapped $Y_Z^\bullet$ radical begins to disappear as the temperature is again raised above 200 K with half the $Y_Z^\bullet$ lost after a 30-s incubation at 253 K (*12*). In intact PSII membranes, Y_Z oxidation occurs at temperatures as low as 5 K (*31*, *32*).

To clarify these issues, it would be useful to work with PSII preparations containing one or two firmly bound manganese ions (i.e., a partially formed Mn-cluster/Y_Z complex with perhaps some properties found in native PSII material). However, only tetrameric Mn preparations [native or photoactivated (*33*, *34*)] or PSII preparation depleted of Mn are commonly available [although extraction of two Mn cations from the OEC is possible, the remaining two must be stabilized (*35*)]. In this context, the interaction of Fe(II) with the high-affinity Mn-binding (HA_Z) site(s) of PSII was of great potential interest (*36*, *37*). The mutually exclusive interaction of Fe(II) and Mn(II) cations with the HA_Z site was originally recognized using the DPC-inhibition assay in a series of kinetic studies (*38*). However, we recently found that incubation of Mn-depleted PSII membranes with Fe(II) under weak light [PSII(−Mn, +Fe) preparations] for a short period of time (in a process similar to photoactivation) leads to the light-dependent oxidation of Fe(II) and the formation of an iron cluster with $2 \leq n \leq 4.5$ (*23*). Thus, after incubation, the interaction of one iron cation with the donor side of PSII(−Mn) membranes is accompanied by the creation of a new Fe-binding site (*37*). The resultant purported iron cluster that is formed blocks the donation of electrons to $Y_Z^\bullet$ from a number of exogenous electron donors [i.e., DPC, Mn(II), Fe(II)] (*37*) and shifts the pK_{app} of the hydrogen bond partner for Y_Z to more acidic pH (*23*). Modification of these properties (the accessibility of $Y_Z^\bullet$ for exogenous donors and the shift of the pK_{app}) by the coordination of Fe(III) indicates that properties assigned to the donor side of intact PSII material are partially reconstituted by iron cations bound to PSII(−Mn) membranes.

In the current paper, we have continued to investigate the effects of bound iron cations on the properties of the donor side of PSII and have now measured (a) the activation energy for the reduction of $Y_Z^\bullet$ during charge recombination between $Y_Z^\bullet Q_a^{\bullet-}$ and (b) the temperature dependence of $Y_Z^\bullet$ reduction by EPR techniques in both PSII(−Mn) and PSII(−Mn, +Fe) membranes. Our data show that blocking the HA_Z Mn-binding site in PSII(−Mn) membranes with Fe(II) is accompanied by the formation of a low barrier hydrogen bond (LBHB) between Y_Z and base B. As such, we infer that the high rate of electron transport from Y_Z to $P680^+$ in intact PSII membranes is determined by the existence of an LBHB between Y_Z and base B, consistent with the results of Zhang and Styring (*32*).

MATERIALS AND METHODS

Biological Samples. BBY-type, PSII-enriched membrane fragments were prepared from market spinach (*37*) and resuspended in buffer A (50 mM MES/NaOH, pH 6.5, 15 mM NaCl, and 0.4 M sucrose). Chlorophyll concentrations and Chl *a*/*b* ratios were determined in 80% acetone, according to the method of Porra et al. (*39*). The rate of O_2 evolution by the PSII membranes was 400−500 μmol of O_2 mg of Chl^{-1} h^{-1}, and the membranes were stored under liquid nitrogen until use. Manganese depletion was accomplished by incubating thawed PSII membranes (0.5 mg of Chl/mL) in 1 M Tris-HCl buffer (pH 9.4), containing 0.4 M sucrose, for 30 min at 5 °C in room light (*40*).

Iron Solutions. Concentrated stocks of 0.5 mM $FeSO_4$ in double-distilled water were made up just prior to an experiment. Little oxidation of Fe(II) in the stock solution (pH 5.6) was observed after 5 h at room temperature. In contrast, the stability of Fe(II) decreased in buffer A (pH 6.5), but only about 5% of the Fe(II) was oxidized after 1 h of incubation (*37*).

Buffers and pH Measurements. Determinations of activation energies in PSII(−Mn) membranes were done in buffer A (pH 5.5 and 6.5) and in Tricine buffer containing 50 mM Tricine/NaOH (pH 8.2), 15 mM NaCl, and 0.4 M sucrose. No differences in the decay kinetics of the samples in either MES or Tricine were observed if the buffers were poised at the same pH (pH 7.0) (*23*). Iron-blocked PSII(−Mn) membranes [note that Fe-blocking of PSII(−Mn) membranes was performed in buffer A at pH 6.5 prior to examination at other pHs] were examined using MES buffer (50 mM MES/NaOH, 15 mM NaCl, and 0.4 M sucrose) at pHs of 5.5, 6.5, and 8.2. Tricine was not used at pH 8.2 because it can destabilize iron cations bound at the HA_Z site (*23*). The pHs of samples resuspended in MES buffer outside of its optimal buffering capacity (i.e., pH < 5.5 or > 7.0) were confirmed directly after addition of all reaction components. The pDs of the buffers prepared in D_2O were determined using the following correction factor: $pD = pH_{meter\ reading} + 0.4$ (*10*, *24*, *41*). The effects of pH on flash-probe fluorescence yield decay kinetics in PSII(−Mn, +Fe) membranes blocked in D_2O were also determined in MES buffer A at all pHs.

Blocking of the HA_Z Mn-Binding Site. PSII(−Mn) membranes (25 μg of Chl/mL) were incubated in buffer A (pH 6.5) with 5 μM Fe(II) under cool white fluorescent room light (4 μEinsteins m^{-2} s^{-1}, PAR) for 2 min at room temperature, pelleted by centrifugation (15000g × 10 min), and resuspended in buffer A (pH 6.5) at a concentration of 1 mg of Chl/mL. For D_2O measurements, we incubated PSII(−Mn) membranes (25 μg of Chl/mL) in buffer A prepared in D_2O (pD 6.5) with 12.5 μM Fe(II) [although concentrations of Fe(II) down to 5 μM for 25 μg of Chl/mL samples can be also used without affecting the results] as above, and resuspended the membranes in D_2O buffer A (pD 6.5) at a concentration of 1 mg of Chl/mL. Experimental measurements were done in H_2O buffers at the indicated pHs.

Flash-Probe Fluorescence Measurements. The decay of the flash-probe fluorescence yield was measured using a home-built instrument capable of 100 μs time resolution (*37*, *42*). Samples, containing 25 μg of Chl/mL (ca. 0.12 μM PSII centers) and 40 μM DCMU in buffer A, were dark-adapted prior to each measurement. In all experiments, excluding those done at room temperature (21−22 °C), temperatures were detected directly in the cuvette using a thermometer probe attached to a pH-meter. Fluorescence data analysis used Data Translation Global Lab software and a DT2839 A/D board mounted in an ALR 486 PC (*42*). Halftimes for the fluorescence decay kinetics were determined from the decay curves. Fluorescence decay kinetics approximated by a single (fast) exponential component were calculated using the equation, $y = y_0 + a_f e^{-k_f t}$. In the case of PSII(−Mn) or PSII(−Mn, +Fe), the samples were measured at pH 5.5, but PSII(−Mn) samples were also measured at pH 6.5 (*23*). Fluorescence decay kinetics of PSII(−Mn, +Fe) samples measured at pH 6.5 or PSII(−Mn) samples measured at pH 8.2 were approximated using the equation, $y = y_0 + a_f e^{-k_f t} + a_s e^{-k_s t}$, because two decay components (fast and slow) provided a better fit to the data (*23*).

EPR Measurements. EPR spectra were recorded on a RE1307 spectrometer (SCB AS USSR) fitted with a nitrogen gas-flow cryostat. A finger-type Dewar was used for measurements at 77 K. PSII(−Mn) and PSII(−Mn, +Fe) membranes were measured in buffer A containing 0.6 mM potassium ferricyanide. During the blocking process, PSII(−Mn) membranes (50 μg of Chl/mL) were incubated in H_2O or D_2O buffer A with 10 μM Fe(II) for 3 min under room light. After that, the samples were centrifuged and resuspended at the indicated concentrations. The spectrometer settings were as follows: microwave frequency, 9.25 GHz; microwave power, 0.2−0.7 mW; modulation amplitude, 3G; modulation frequency, 100 kHz; time constant, 100 ms; sweep time, 15 s. Time-resolved EPR spectra were accumulated over 10−30 scans. The procedure used for trapping the $Y_Z^{\bullet}$ radical was performed as in ref *12*: EPR tubes with membrane samples were placed at the top of a transparent dewar, half-filled with liquid nitrogen, and illuminated with white saturating light provided by a 300-W projector lamp (KGM-300). During illumination, the tubes were lowered toward the surface of liquid nitrogen. After 20−30 s, the samples were plunged into the liquid nitrogen, and the light was turned off after a few more seconds. The procedure for determining $Y_Z^{\bullet}$ radical content in the EPR spectra is described in the figure legends that specifically present EPR data.

RESULTS AND DISCUSSION

To gain a better understanding of the mechanism governing proton-coupled electron transfer between Y_Z and P680, it is essential to determine the contribution of the hydrogen bond to the activation energy of the overall process. To do this, one must calculate the activation energy at two pHs, one at alkaline pH where the hydrogen bond exists and the other at acid pH where the bond between Y_Z and base B is absent. Several studies of temperature effects on the rate of Y_Z oxidation in PSII(−Mn) membranes have been reported at individual pHs. For example, Reinman and Mathis studied the reduction of $P680^+$ in Tris-washed thylakoid membranes using an optical method (*43*), as did Renger and co-workers with PSII(−Mn) membranes (*44*). Ahlbrink et al. (*15*) expanded upon these studies by working with PSII(−Mn) core particles between 0 and 25 °C at different pHs, and Shigemori et al. (*30*) used EPR techniques to examine the reduction of $Y_Z^{\bullet}$ (i.e., $Y_Z^{\bullet}$ Q_a^- charge recombination) at different pHs between −50 and 24 °C.

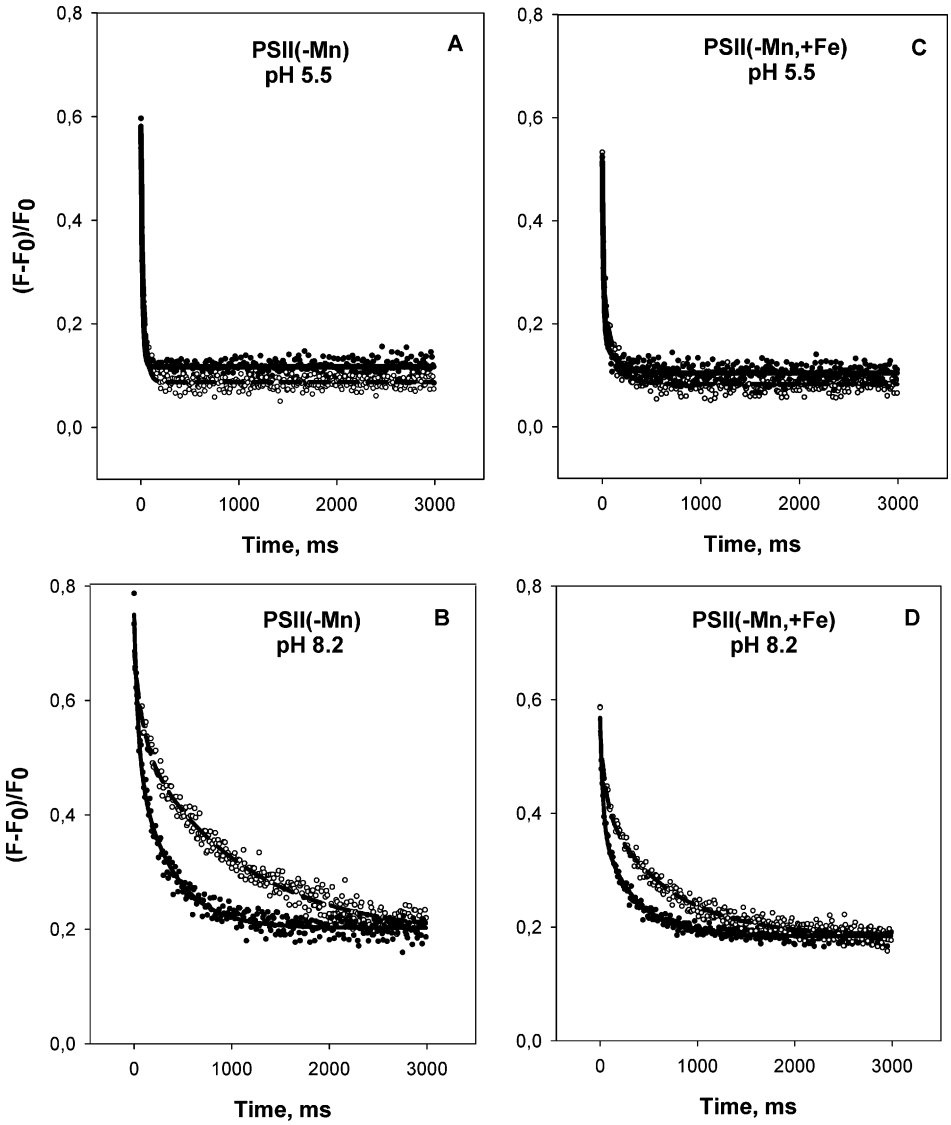

FIGURE 1: The effect of temperature on the kinetics of flash-probe fluorescence decay profiles due to charge recombination between Q_a^- and $Y_Z^\bullet$ in PSII(−Mn) and PSII(−Mn, +Fe) membranes at pHs 5.5 and 8.2. The experimental conditions were as follows: (i) 25 μg of Chl/mL of PSII(−Mn) membranes and 40 μM DCMU were added to buffer containing 50 mM Tricine/NaOH (pH 8.2) or 50 mM MES/NaOH (pH 5.5) buffer, 15 mM NaCl, and 0.4 M sucrose and (ii) 25 μg of Chl/mL of PSII(−Mn, +Fe) membranes and 40 μM DCMU were added to buffer containing 50 mM MES/NaOH (pH 5.5 and 8.2), 15 mM NaCl, and 0.4 M sucrose (see Materials and Methods for details). The fluorescence decay kinetics were fit with one (pH 5.5) or two (pH 8.2) exponentials as discussed in ref *23*. Solid and open circles in the figures indicate actual data points, and the solid and dashed curves are fits to the data. Each curve in figures represents the average of 2−4 fluorescence decays measured at the temperatures indicated below: (A) 8.3 °C (open circles and dashed line) and 21 °C (solid circles and solid line); (B) 6.6 °C (open circles and dashed line) and 21 °C (solid circles and solid line); (C) 8.1 °C (open circles and dashed line) and 20.4 °C (solid circles and solid line); (D) 8.8 °C (open circles and dashed line) and 21 °C (solid circles and solid line).

In past studies (*23*, *37*, *42*), we used flash-probe fluorescence methods to measure the rate of $Y_Z^\bullet$ reduction during the process of charge recombination between $Y_Z^\bullet$ and Q_a^-, as have several other laboratories (*22*, *26*, *45*, *46*). Because of the possibility of energy transfer between different PSII centers, the relationship between the concentration of Q_a^- and the fluorescence yield can be nonlinear (*47*). However, this effect can be minimized if divalent cations are removed from the buffer during assay (*48*). Furthermore, a recent comparative analysis of the halftimes obtained for $Y_Z^\bullet$ reduction by flash-probe fluorescence and those obtained by EPR and optical spectroscopies have shown little difference when using spinach PSII materials (*23*).

The effect of temperature on the flash-probe fluorescence decay curves measured in PSII(−Mn) and PSII(−Mn, +Fe) membranes at acidic (5.5) and alkaline (8.2) pHs is shown in Figure 1. Cooling of the membrane samples from room temperature to about 8 °C is accompanied by a decrease in the rate of charge recombination in both kinds of samples. However, the effect of temperature is more pronounced on a relative basis at alkaline pHs (pH > pK_{app}) where the phenolic hydrogen of Y_Z is involved in the formation of a hydrogen bond with base B (Figure 1B,D). At acidic pHs (pH < pK_{app}) the hydrogen bond is absent, and the influence of temperature on the recombination rate is weaker (Figure 1A,C). Besides pH and temperature influences on the rate of charge recombination, the effects of blocking iron cations on F_{max} were also observed (Figure 1C,D). The binding of iron cations to the high-affinity Mn site is accompanied by a 20−25% decrease in F_{max} as compared to control, Mn-depleted membranes. Preliminary studies have shown that this effect is caused primarily by the binding of iron cations

Table 1: Results of Exponential Fits to the Fluorescence Decays at Room Temperature[a]

	fast component		slow component		offset
sample	A_f (%)[b]	$t_{1/2}$ (ms)	A_s (%)	$t_{1/2}$ (ms)	A_o (%)
		PSII(−Mn)			
pH 5.5	79 ± 4[c]	11 ± 1	0	0	21 ± 4
pH 6.5	75 ± 2	35 ± 3	0	0	25 ± 2
pH 8.2	32 ± 1	28 ± 2	42 ± 1	239 ± 16	26 ± 2
		PSII(−Mn, +Fe), blocked in H_2O			
pH 5.5	78 ± 2	15 ± 1	0	0	22 ± 2
pH 6.5	32 ± 3	15 ± 1	41 ± 5	38 ± 4	27 ± 7
pH 8.2	34 ± 1	20 ± 3	33 ± 0	231 ± 15	33 ± 1
		PSII(−Mn, +Fe), blocked in D_2O			
pH 5.5	50 ± 5	6 ± 1	31 ± 4	46 ± 6	19 ± 3
pH 6.5	49 ± 3	16 ± 2	31 ± 3	115 ± 2	20 ± 1
pH 8.2	41 ± 2	26 ± 25	32 ± 2	247 ± 18	27 ± 1

[a] Data were fitted to one or a sum of two exponentials and offset. [b] Amplitudes (A) of the exponents are expressed in percentage of the total amplitude. [c] Arithmetic means and standard deviations of 3−4 separate measurements conducted on the different samples are tabulated. The fitting procedure was done with a significance level $\alpha \leq 0.05$.

and not by the photooxidation of PSII reaction centers during incubation of the membranes with iron in the light. A decrease in F_{max} was also found during incubation of PSII-(−Mn) membranes with Mn(II). The reason for this effect is now under investigation using continuous and flash sources of light.

Measurements similar to those in Figure 1 were also performed at pHs 5.5, 6.5, and 8.2 in both PSII(−Mn) and PSII(−Mn, +Fe) membranes at a number of temperatures between 6 and 22 °C to determine the activation energies of charge recombination. The decay kinetics can be fit with either one or two exponentials with the offset depending on the pH (*23*) as described in Materials and Methods. The results of fitting the decay kinetics measured at room temperature are shown in Table 1, and the changes in the amplitudes of the fast and slow phases with temperature in control and blocked PSII(−Mn) membranes are shown in Figure 2. At pH 5.5, only one exponential phase (fast) is present in the fluorescence decay kinetics, and the temperature effect on the amplitude of this phase is minimal (see inserts on Figure 2A−C). At alkaline pH (8.2), an additional slow decaying component appears. The amplitude of the slow component appears to increase with temperature proportionally to the decrease in fast component contribution to the total fluorescence amplitude. The offsets are temperature independent (results not shown). The amplitudes of the fast and slow components and the offsets are interrelated such that their sum (F_{max}) remains constant over the range of temperatures studied. As seen in Figure 2, the intersection points of the lines approximating the experimental data are different for the control and blocked PSII(−Mn) membranes. The exact position of this point is determined by the different yields of fluorescence (F_{max}) in the two types of membranes. In control PSII(−Mn) membranes, F_{max} exceeds that of blocked membranes by about 20% (see above). Thus, the difference between the amplitudes of fast and slow components at low temperatures is larger in unblocked membranes and intersection point shifts toward higher temperatures.

The lifetimes of the fitted exponentials ($t_{1/2}$ measured at the room temperature in different samples at pHs 5.5, 6.5, and 8.2 are shown in Table 1) are also temperature

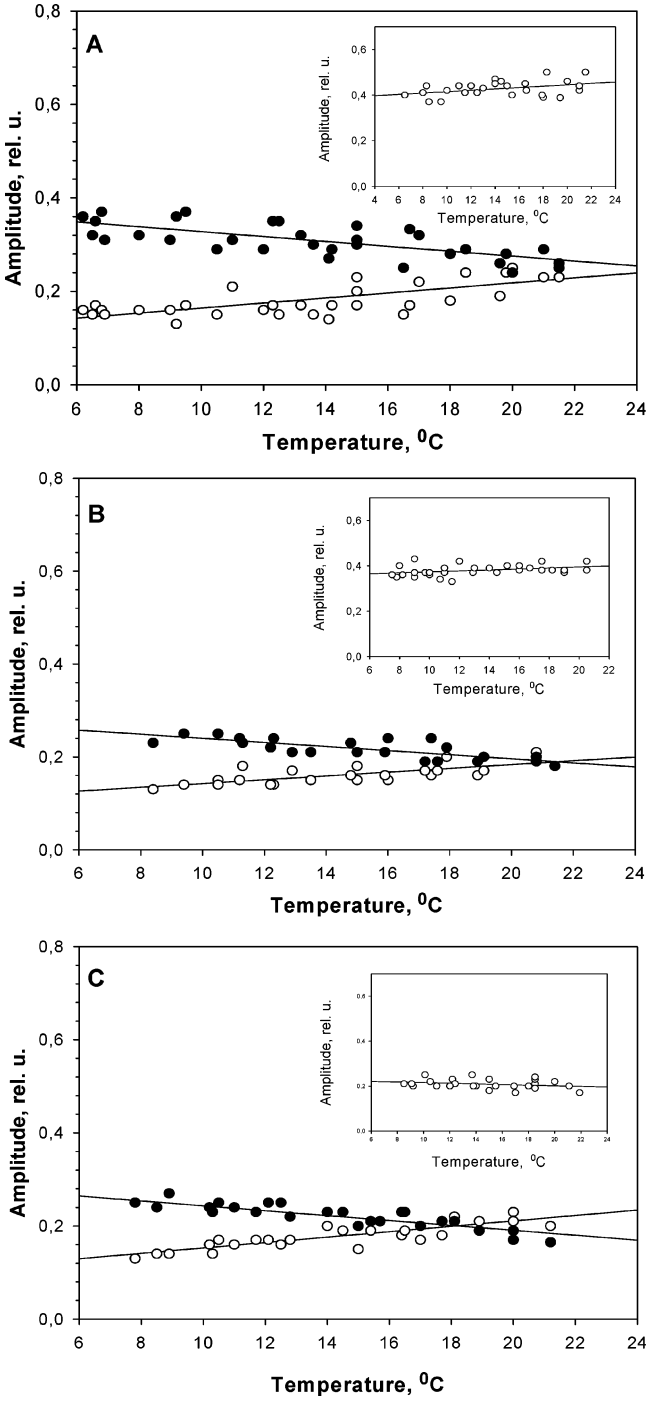

FIGURE 2: The amplitudes of the slow (●) and fast (○) components of flash-probe fluorescence decay profiles as a function of temperature at pH 8.2 in PSII(−Mn) membranes (A), Mn-depleted, Fe-blocked in H_2O PSII membranes (B) and Mn-depleted, Fe-blocked in D_2O PSII membranes (C). Insets: Corresponding dependencies of the fast component amplitudes measured at pH 5.5.

dependent, and their values were used to determine the activation energies (E_a) of charge recombination. Examples of Arrhenius plots used for E_a determinations are presented in Figure 3 and numerical data for many such plots are shown in Table 2. Table 2 shows that at pH 5.5, where the fluorescence decays are described by only a single (fast) exponential phase, the E_a's for PSII(−Mn) and PSII(−Mn, +Fe) membranes are equal to 42.2 ± 2.9 and 46.4 ± 3.3 kJ/mol, respectively. The difference between these E_a values is very small and statistically insignificant (according to the

Table 2: Activation Energies of the Fast and Slow Components of $Y_Z^{\bullet}Q_a^-$ Recombination (kJ/mol) at Different pHs in PSII(−Mn) Membranes or in Mn-Depleted PSII Membranes Where the HA_Z Mn-Binding Site Was Blocked with Iron Cations in H_2O or D_2O Buffer A (pL 6.5[a])

	sample					
	PSII(−Mn)		PSII(−Mn, +Fe) (blocked in H_2O)		PSII(−Mn, +Fe) (blocked in D_2O)	
	components		components		components	
pH	fast	slow	fast	slow	fast	slow
5.5	42.2 ± 2.9 (3)[b]		46.4 ± 3.3 (4)		44.3 ± 10.4 (3)	49.7 ± 0 (3)
6.5	41.8 ± 2.5 (3)		46.4 ± 11.7 (3)	36.1 ± 7.5 (5)	44.3 ± 15 (3)	47.2 ± 9.6 (3)
8.2	43.5 ± 12.5 (4)	48.1 ± 1.7 (4)	50 ± 0 (2)	36.4 ± 1.3 (3)	44.3 ± 10 (3)	42.6 ± 0.4 (3)

[a] During the E_a experiments, the temperatures of the samples were measured with a thermometer probe and noted at the beginning of the fluorescence decay measurements. Usually for one Arrhenius plot 8−12 fluorescence decays were measured at different arbitrary temperatures in the range of 6−22 °C. The number of Arrhenius plots used for determining the arithmetic means of the E_a is given in brackets in the table. [b] Values in parentheses indicate the sample size.

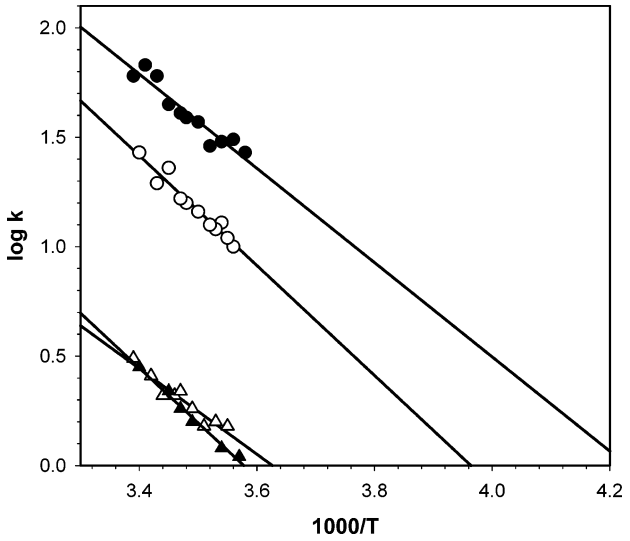

FIGURE 3: Arrhenius plots of the rates of $Y_Z^{\bullet}Q_a^-$ recombination in PSII(−Mn) membranes (solid symbols) and PSII(−Mn, +Fe) membranes (open symbols) measured at pH 5.5 (circles, fast component) and 8.2 (triangles, slow component). See legend to Table 2 for other experimental conditions.

t-test at the standard significance level $\alpha = 0.05$). Increasing the pH is accompanied by the deprotonation of base B, the formation of a hydrogen bond between Y_Z and the deprotonated form of base B and the appearance of the slow component in the fluorescence decay. The amounts of slow component are significant at pH > 8 in PSII(−Mn) membranes ($pK_{app} = 7.1$) and at pH > 6.5 in blocked PSII(−Mn, +Fe) membranes ($pK_{app} = 6.1$) (*23*), but they never reach 100% even at pHs greater than 2 units above the pK_{app}. The activation energies of the slow components were also determined from Arrhenius plots (*49*) such as in Figure 3 (triangles), and the numerical values are also shown in Table 2. The E_a's for the slow components at pH 8.2 are 48.1 ± 1.7 kJ/mol in PSII(−Mn) membranes and 36.4 ± 1.3 kJ/mol in PSII(−Mn, +Fe) membranes. Thus, blocking the HA_Z Mn-binding site with iron decreases the E_a for $Y_Z^{\bullet}$ reduction when Y_Z is hydrogen-bonded to base B. The difference between the E_a's for the slow components in PSII(−Mn) and PSII(−Mn, +Fe) membranes is not large (about 25%; see Table 2 and Figure 3), so we performed statistical t-tests to determine if the difference was significant. The test was performed at the standard significance level, $\alpha = 0.05$, for arithmetic means of 48.1 and 36.6, standard deviations 1.7 and 1.3, and sample sizes indicated in Table 1. The results showed that the difference is statistically significant at the 0.001 level.

The E_a values shown in Table 2 are consistent with those found by some authors who studied PSII(−Mn) samples but are different from those reported by other groups. This discrepancy can be explained by either the type of preparation or the type of reaction examined (i.e., Y_Z oxidation or $Y_Z^{\bullet}$ reduction). For example, Shigemori et al. (*30*) studied the fast component of $Y_Z^{\bullet}$ and Q_a^- recombination (i.e., $Y_Z^{\bullet}$ reduction) and found an E_a of 41.8 kJ/mol at pH 8.0. This value is similar to our results for charge recombination in Mn-depleted membranes (Table 2). For Y_Z oxidation, Reinman and Mathis reported an E_a of 47.7 kJ/mol at pH 7.0 (in Mn-depleted thylakoids, the decays were fit with a single exponential) (*43*), Renger et al. (*44*) measured a value of 27.2 kJ/mol in Tris-washed PSII membrane fragments at pH 6.5, and Jeans et al. (*50*) found a value of 33 kJ/mol in hydroxylamine-treated BBYs preparations from spinach at pH 6.5 (the decays were fit with one exponential on a short time scale). Ahlbrink et al. (*15*) found that the E_a for Y_Z oxidation decreased with increasing pH as the hydrogen bond formed. Their results showed that base B had an apparent p*K* of 7.0, and they measured E_a's of 28.8 kJ/mol at pH 5.0 for the slow kinetic component and 14.4 kJ/mol at pH 8.0 for the fast kinetic component. These data show that Y_Z oxidation in PSII membranes requires somewhat less activation energy than tyrosine radical reduction in charge recombination. This value is around 30 kJ/mol at pH 6.5. The E_a value observed by Reinman and Mathis is larger perhaps because in their experiments they used thylakoids rather than PSII membranes (*43*).

As was shown previously (*23*), blocking the HA_Z Mn-binding site with iron cations decreases the pK_{app} for $Y_Z^{\bullet}$ reduction, but Table 2 shows that it also decreases the activation energy of the slow component of the fluorescence decay profile compared to PSII(−Mn) membranes. Since the slow decay component reflects $Y_Z^{\bullet}$ reduction in reaction centers with a hydrogen-bonded Y_Z, we suggest that Fe-blocking may change (at least partially and perhaps not in all reaction centers) the strength of the hydrogen bond controlling electron transfer via Y_Z.

The suggestion that the hydrogen bond between Y_Z and base B should be strong to facilitate the high rate of Y_Z oxidation in O_2-evolving PSII preparations has already been discussed (*17*, *24*, *51*, *52*). However, Zhang and Styring, considering the possible mechanism for Y_Z oxidation at 5

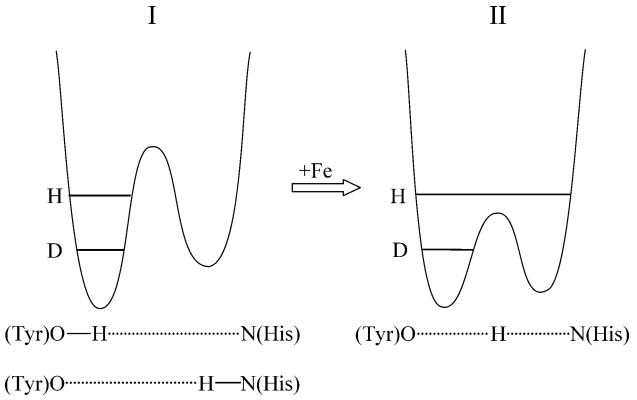

FIGURE 4: The potential energy functions for a weak, double-well (I) and a strong, low-barrier (II) hydrogen bond. The horizontal lines give the zero-point vibrational energy levels of protium (H) and deuterium (D). O and N are a proton donor (D1-Tyr161) and acceptor (D1-His190), respectively. PSII(−Mn) membranes have an aqueous microenvironment around Y_Z ($Y_Z^\bullet$ is accessible to water molecules) (*10*, *12*), and Y_Z forms a weak hydrogen bond (I). The binding of iron cations to the HA_Z Mn-binding site is accompanied by a compression of the protein structure around Y_Z and blocking of the access of a number of exogenous electron donors to $Y_Z^\bullet$ (*33*), possibly due to squeezing out water from the space around Y_Z (see Results and Discussion). Formation of a LBHB (II) probably occurs due to the shortening of the distance between Y_Z and D1-His190 and the transition of the Y_Z environment to a more hydrophobic state.

K, suggested recently that the phenolic proton of Y_Z might be involved in a strong bond with base B resembling a LBHB (*32*).

In Figure 4 we show potential energy curves to demonstrate the difference between a weak hydrogen bond and LBHB. Weak hydrogen bonds predominate in proteins and nucleic acids, have a length of about 2.7−3.0 Å, and the energy of the bond varies between 2 and 20 kJ/mol (*53*). The proton in Figure 4(I) is bonded covalently to atom (O) and attracted electrostatically to second electronegative atom (N). The proton has two alternative locations or free energy wells corresponding to a covalent bond with either O or N. The length of a LBHB [Figure 4(II)] ranges from 2.45 to 2.65 Å, and the $\Delta H_{formation}$ increases to 63−84 kJ/mol (*54*). As the overall O − N distance decreases, the energy barrier between the two proton wells also decreases significantly. When the barrier height approaches the zero-point vibrational energy level of hydrogen, the proton delocalizes and can now move freely between the proton acceptor and donor (*55*). Thus, the formation of a strong hydrogen bond with a low energy barrier between Y_Z and base B (D1-His190) could explain the low activation energy required to shift the hydrogen along the hydrogen bond from base B to $Y_Z^\bullet$ during the reduction of $Y_Z^\bullet$.

Although a proton becomes delocalized in the LBHB, a heavier deuterium will occupy a lower zero-point vibrational energy level. In this case as illustrated in Figure 4(II), an activation energy barrier could still exist for shifting the deuterium between the donor and acceptor species (*56*). Thus, the substitution of deuterium for hydrogen in the LBHB should partially reverse those sample properties that are determined by the existence of the hydrogen bond. Furthermore, the high strength of the LBHB (*54*) should result in the slow exchange rate of protons in the LBHB with solvent protons (*57*). Therefore, one can expect that incubating PSII membranes containing a LBHB in D_2O would not be accompanied by extensive H_{LBHB}/D exchange. Indeed, data on H/D isotope exchange effects in O_2-evolving (possibly having a strong hydrogen bond between Y_Z and base B, see ref *32*) (*17*, *24*, *32*, *51*) and PSII(−Mn) (weak hydrogen bond or absence of a hydrogen bond) (*10*, *15*, *19*, *24*, *44*) preparations supports this suggestion. Renger and co-workers found that in intact PSII preparations, the rate of Y_Z oxidation by $P680^+$ is not affected significantly by exchanging deuterium for protons (*58*), whereas in PSII(−Mn) preparations, the rate of Y_Z oxidation shows a large deuterium effect (2−3 times) (*10*, *19*, *44*). Moreover, in PSII(−Mn) samples, H/D exchange in the immediate proximity to $Y_Z^\bullet$ occurs rapidly, either during the time it takes to prepare the sample (<10 min) for measurement (*10*) or with a $\tau < 1$ min (*44*).

Besides merely incubating PSII(−Mn, +Fe) membranes in D_2O, there is perhaps a better way to insert a deuterium ion into the LBHB. If the blocking process is completed by the formation of a LBHB, then blocking PSII(−Mn) membranes with iron ions in D_2O instead of H_2O should facilitate insertion of a deuterium into a LBHB. Thus, when locked in a LBHB, deuterium ions should have a low rate of exchange with solvent H^+ ions, while deuterium ions forming a weak hydrogen bond should have a fast exchange rate (see above). To test this assumption, we incubated PSII(−Mn) membranes with Fe(II) in D_2O instead of H_2O buffer A under illumination (conditions required for the blocking process). After a 2-min incubation [sufficient time to substitute any exchangeable protons with deuterium in Tris-washed PSII membranes (*44*)], the samples were pelleted and then resuspended in a small volume D_2O buffer A (pD 6.5). See the Materials and Methods for more details. Successful Fe-blocking of the HA_Z Mn-binding site with iron was checked at that point by the techniques reported previously (*37*). After dilution of the membranes with buffer A (H_2O), the content of D_2O in a sample was about 2.5%, and measurements were started within 2−3 min. These experimental conditions suggest that protons should substitute successfully for any exchangeable deuterium ions before the beginning of the measurement.

The results in Figure 5 show that the pH dependence for the $t_{1/2}$ of charge recombination in PSII(−Mn, +Fe) membranes blocked in D_2O has a pK_{app} of about 7.6. By way of explanation, 7.6 is an apparent pK since it was determined by plotting $t_{1/2}$ vs pH rather than plotting the rate constant k vs pH. Thus, it reflects only the effect of iron on the rate of $Y_Z^\bullet$ reduction. Furthermore, the pH dependence curve does not saturate at pH 8.0 in Figure 5. In fact, experiments at more alkaline pHs (to determine such a saturation point) could not be done since extraction of bound iron occurs at high pH (*23*). Therefore, the actual pK_{app} might be somewhat higher than 7.6.

Nevertheless, the 7.6 pK_{app} value is significantly higher than the pK_{app} = 6.1 found for PSII(−Mn, +Fe) membranes blocked in H_2O (*23*) but closer to the pK_{app} of 7.1 found in control, unblocked PSII(−Mn) membranes (*23*). The difference between the two pK_{app}'s (7.6 and 7.1) can be explained by the fact that the inflection point for an acid/base system with D^+ instead of H^+ shifts to more basic pHs by 0.5−0.6 units (*41*). Thus, the equivalent pK_{app} of base B with H^+ substituted for D^+ is equal to 7.6−0.5(0.6) = 7.1(7.0). This agrees very well with the measured pK_{app} of base B (7.1) in

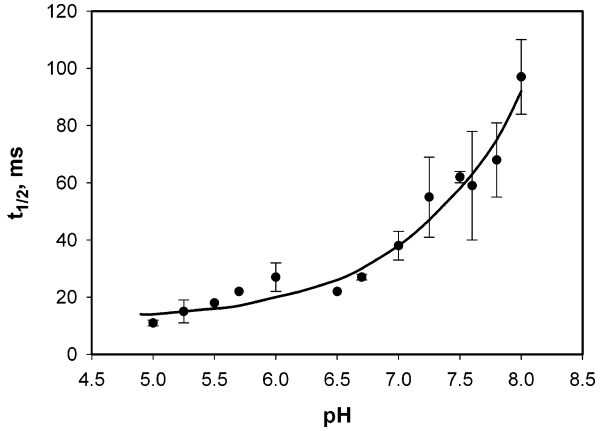

FIGURE 5: The pH dependence of the apparent halftimes for charge recombination between $Y_Z^\bullet$ and Q_a^- in PSII(−Mn, +Fe) membranes. Blocking of the HA_Z Mn-binding site with iron was performed in D_2O-buffer A (pD 6.5) as described in the Materials and Methods. After blocking was done, the PSII membranes were pelleted by centrifugation, resuspended at 1 mg of Chl/mL in D_2O-buffer A (pD 6.5), and kept on ice in the dark until use. The experimental conditions during flash-probe fluorescence decay measurements were as follows: 25 μg of Chl/mL and 40 μM DCMU in H_2O-buffer A (50 mM MES/NaOH, 15 mM NaCl, and 0.4 M sucrose) at the indicated pH. The assays themselves were performed in buffer containing water rather than D_2O. See Materials and Methods for additional information.

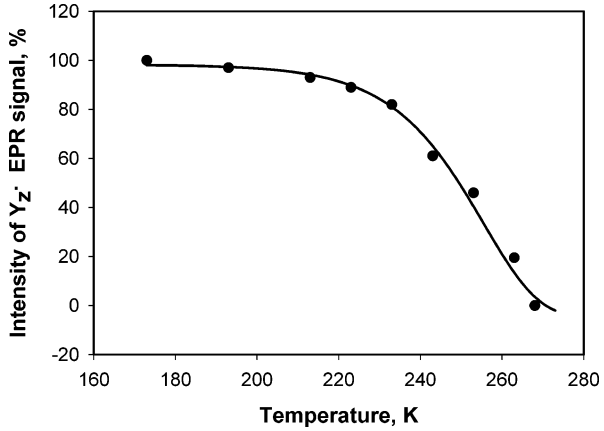

FIGURE 6: Temperature dependence of the stability of trapped $Y_Z^\bullet$ EPR signal (SII_f) in PSII(−Mn) membranes as the temperature is raised. The radical signal was determined from light-minus-dark EPR difference spectra [i.e., the spectrum of an illuminated sample with a trapped $Y_Z^\bullet$ EPR signal and fully oxidized $Y_D^\bullet$ radical ("light" spectrum) minus the spectrum of a sample dark-adapted at 268 K ("dark" spectrum)]. Since "dark" EPR spectra contain only a $Y_D^\bullet$ EPR signal due to the high stability of the $Y_D^\bullet$ radical (see Figure 7) and rapid reduction of both the $Y_Z^\bullet$ and $Chl_Z^\bullet$ radicals at 268 K, the light-minus-dark difference EPR spectra do not contain a $Y_D^\bullet$ EPR signal contribution. Therefore, they can be used to determine the $Y_Z^\bullet$ radical content in the samples. Specifically, the EPR spectrum of a sample frozen under saturating light conditions was first measured in the dark at 173 K. Subsequently, the sample was warmed to the indicated temperature, incubated at this temperature for 1 min in the dark, and then rapidly cooled to 173 K. At this point, a measurement of the $Y_Z^\bullet$ EPR signal was done again. The EPR spectrum of the dark-adapted sample was measured as follows: the sample was cooled under illumination to 173 K, warmed to 268 K, dark-adapted for 1 min, frozen again to 173 K, and the EPR spectrum was measured at 173 K. The sample concentration was 2.5 mg of Chl/mL, and the number of EPR spectrum scans varied from 10 to 20.

PSII(−Mn) membranes (*23*). These results also support the suggestion that the shift of pK_{app} of $Y_Z^\bullet$ reduction (from 7.1 to 6.1) due to blocking of the HA_Z site by iron cations (*23*) is determined by the formation of a LBHB with little or no barrier for the movement of a proton along the hydrogen bond. Furthermore, our results show that the substitution of deuterium for hydrogen in PSII(−Mn, +Fe) membranes reverses the effect of iron blocking due to the existence of an energy barrier for the movement of a deuteron inside the LBHB. This provides additional support for the idea that electron transport from $Y_Z^\bullet$ in intact membranes is regulated by a LBHB between Y_Z and base B. As seen in Table 2, PSII(−Mn, +Fe) samples blocked in D_2O exhibit an increase in the E_a of the slow component from 36.1 to 36.4 to 42.6−47.2 kJ/mol. These E_a values are also similar to unblocked PSII(−Mn) membranes (48.1 kJ/mol, Table 2). However, not all the properties of PSII(−Mn) membranes blocked in D_2O correspond to those of unblocked PSII(−Mn) samples. Besides the increase in E_a value of the slow component at pH 8.2, H^+/D^+ exchange has an additional effect on charge recombination. Tables 1 and 2 show that a slow component appears in samples blocked in D_2O at acidic pH's (5.5 and 6.5), which is not seen in unblocked PSII(−Mn) membranes. The reason for this is not known. Undoubtedly, the interaction of a proton with a proton acceptor and donor inside a weak hydrogen bond with a length of 2.7−3.0 Å should differ from the behavior of deuterium, having larger mass inside a shorter (2.5−2.6 Å), strong hydrogen bond. The difference might not only be the appearance of activation barrier.

The oxidation of Y_Z in PSII(−Mn) membranes is significantly delayed or does not take place at temperatures below 230−250 K (*24*, *29*, *30*), and the reduction of trapped $Y_Z^\bullet$ occurs over the same temperature range (*12*). However, in intact PSII membranes, the oxidation of Y_Z can occur at 5 K (*31*, *32*). Since the $Y_Z^\bullet$ radical should be deprotonated during oxidation, and proton movements in normal weak hydrogen bonds (i.e., in water or ice) are severely restricted at temperatures below 100 K (*59*), Zhang and Styring (*32*) suggested that proton movements at very low temperatures in intact PSII membranes are due to the existence of an LBHB between Y_Z and base B.

From our results above and those of Zhang and Styring (*32*), we would predict that in Fe-blocked PSII(−Mn) membranes, the Y_Z "freezing" temperature (the temperature at which only half the Y_Z can be oxidized under illumination during freezing or half the trapped $Y_Z^\bullet$ can be reduced during warming) should be significantly lower than that in PSII(−Mn) membranes. Figure 6 shows that in PSII(−Mn) membranes, half of the trapped $Y_Z^\bullet$ radical disappears by the time the sample is warmed to about 253 K. The amount of $Y_Z^\bullet$ radical was determined at the field position specific for $Y_Z^\bullet$ in light-minus-dark (adapted at 268 K) EPR difference spectra (*24*) (see the arrows in Figure 8). Subtraction of the EPR spectra of samples dark-adapted at 268 K (containing $Y_D^\bullet$ radical only) from EPR spectra measured after freezing the samples under illumination (containing $Y_Z^\bullet$, $Y_D^\bullet$, and some other light-inducible radicals) allows us to plot difference spectra that do not contain a $Y_D^\bullet$ signal, since all radicals except $Y_D^\bullet$ decay quickly during the 1-min dark incubation at 268 K. Although, $Y_D^\bullet$ is stable at 268 K and room temperature in the dark (for a review see refs *1* and *16*), the different pathways for $Y_D^\bullet$ reduction such as the recombination of $Q_a^{\bullet-}$ with $Y_D^\bullet$ are possible (*60*). Moreover,

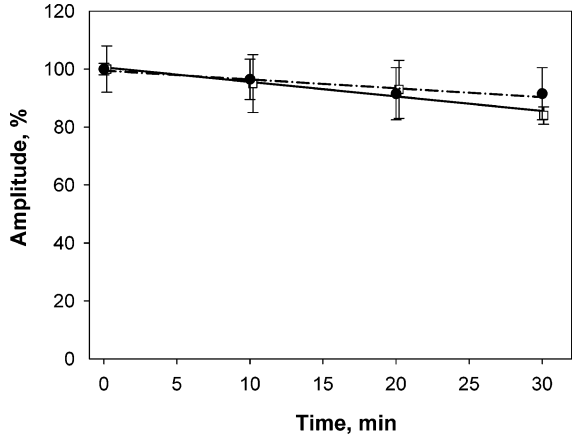

FIGURE 7: Decay of the $Y_D^{\bullet}$ radical in PSII(−Mn) (□) and PSII-(−Mn, +Fe) (●) membranes in the dark at room temperature. The samples were illuminated for 1 min under saturating light at 0−4 °C in the presence of 0.6 mM potassium ferricyanide and then incubated in the dark at room temperature. The first spectrum (time zero) was measured 2 min after concession of illumination. Two samples were measured for each curve. The amount of $Y_D^{\bullet}$ radical was determined at the same field position as $Y_Z^{\bullet}$ radical (indicated by arrow in Figure 8).

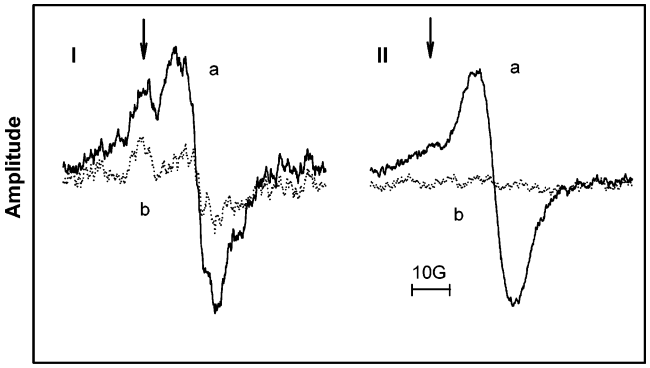

FIGURE 8: $Y_Z^{\bullet}$ EPR spectra recorded at different temperatures in PSII(−Mn) membranes (I) and in PSII(−Mn) membranes with an Fe-blocked HA Mn-binding site (II). All spectra are difference spectra measured as described in the Figure 6 legend. (a) $Y_Z^{\bullet}$ radical content in the sample at 173 K and (b) $Y_Z^{\bullet}$ radical content in the sample at 253 K. Arrows indicate the position of SII_f signal.

the stability of the SII_s signal might be different in PSII(−Mn) and PSII(−Mn, +Fe) membranes due to the effect of bound iron. These factors can influence estimations of the amount of $Y_Z^{\bullet}$ content in different samples. Therefore, we measured the rate of $Y_D^{\bullet}$ decay in PSII(−Mn) samples at room temperature in the dark and compared this rate with that observed in blocked PSII(−Mn) membranes. The samples were illuminated at 0−4 °C and then dark adapted for two minutes before measuring $Y_D^{\bullet}$ decay kinetics to allow for the recombination of unstable radicals (mainly Y_Z). Figure 7 shows that the rate of $Y_D^{\bullet}$ disappearance in both samples is in fact the same and rather slow (only about 5−10% of the $Y_D^{\bullet}$ radical disappears during the 15−20 min it took to obtain the data in Figures 8 and 9). Therefore, the field position indicated by the arrow in Figure 8 for all practical purposes corresponds only to $Y_Z^{\bullet}$ (and not to $Y_D^{\bullet}$), and the value of this maximum can be used to compare the $Y_Z^{\bullet}$ radical content in blocked and unblocked samples. Although there is a small overstatement (5−10%) in the amount of $Y_Z^{\bullet}$ radical that we measure, the same rate of $Y_D^{\bullet}$ radical

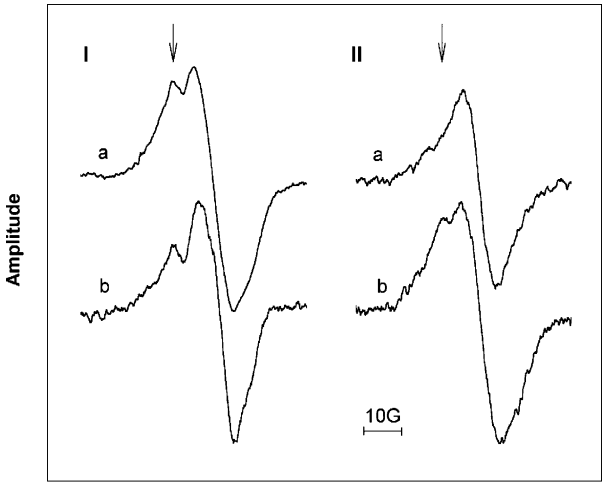

FIGURE 9: Effect of H^+/D^+ exchange on the low-temperature $Y_Z^{\bullet}$ radical spectra from PSII(−Mn) and PSII(−Mn, +Fe) samples: (Ia) PSII(−Mn) membranes; (Ib) PSII(−Mn) membranes that were incubated in D_2O buffer for 3 min, pelleted, and resuspended in H_2O buffer before EPR measurement; (IIa) PSII(−Mn) blocked by iron cations in H_2O buffer; (IIb) PSII(−Mn) membranes blocked by iron cations in D_2O buffer (see the procedure in Materials and Methods). The spectra are difference spectra measured as described in Figure 6 legend except that concentration of the membranes in EPR tubes was 3.5 mg of Chl/mL, the number of EPR scans was 30, spectra of samples were measured at 77 K, and the dark samples were dark-adapted at 293 K.

decay observed in both PSII(−Mn) and PSII(−Mn, +Fe) samples allows us to directly compare the two types of samples. Finally, the 253 K value in Figure 6 found in our spinach PSII membranes coincides closely with that reported for the 50% loss of $Y_Z^{\bullet}$ radical in the *Synechocystis 6803* D2-Tyr160Phe mutant (*12*). The decrease in the amount of trapped $Y_Z^{\bullet}$ radical during the warming process can result from two processes: recombination of $Y_Z^{\bullet}$ with Q_a^- and/or its reduction by the ferrocyanide, reduced by the acceptor side of PSII (*12*, *61*). However, flash-probe fluorescence control experiments (*42*) provide no evidence for the reduction of $Y_Z^{\bullet}$ by 2 mM ferrocyanide (results not shown).

In contrast to our results with PSII(−Mn) membranes [Figures 6 and 8(I)], we did not detect any $Y_Z^{\bullet}$ radical in Fe-blocked PSII(−Mn) membranes either at 173 K [Figure 8(II)) or 77 K (Figure 9(IIa)]. This means that any $Y_Z^{\bullet}$ generated during the freezing process is in fact not trapped, can be re-reduced at 77 K, and might be reduced at even lower temperatures. These data indicate that specifically bound iron cations (*37*) transform the hydrogen-bond net around Y_Z in a way that results in a significant decrease in the Y_Z trapping temperature. We postulate that this transformation modifies the hydrogen bond between the phenolic group of Y_Z and base B by converting it to a LBHB. To prove this, we used the same approach as before (Figure 5 and Table 2), namely, by blocking the HA_Z Mn-binding site in the presence of D_2O, followed by measuring EPR spectra in H_2O buffer. The results demonstrate that the existence of an activation barrier in the LBHB for movement of D^+ leads to an increase in the Y_Z-trapping temperature so that $Y_Z^{\bullet}$ is stable at 77 K [Figure 9(IIb)] as is the case with PSII(−Mn) membranes [Figure 9(Ia and Ib)]. The spectra shown on Figure 9 are light-minus-dark difference spectra, and the original light and dark spectra are represented in the appendix

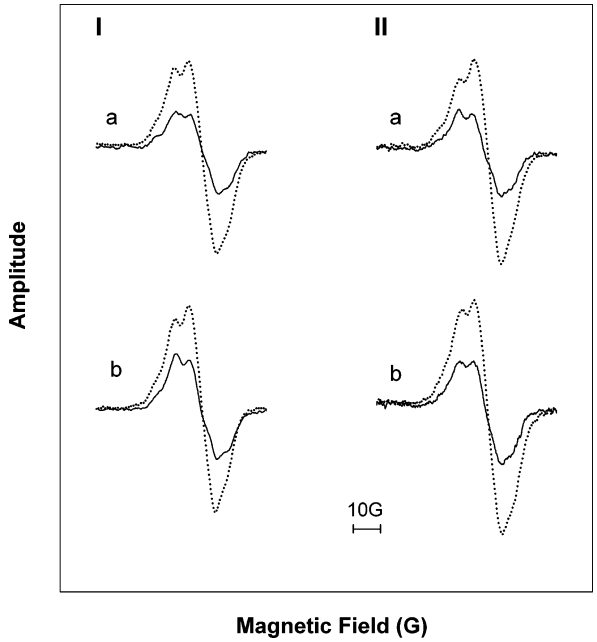

FIGURE 10: EPR spectra from light (dotted lines) and dark (solid lines) treated PSII(−Mn) (I) and PSII(−Mn, +Fe) (II) membranes that were used to calculate the light-minus-dark difference spectra in Figure 9. (Ia) PSII(−Mn) membranes in H_2O buffer; (Ib) PSII(−Mn) membranes that were incubated in D_2O buffer for 3 min, pelleted and resuspended in H_2O buffer before EPR measurement; (IIa) PSII(−Mn) membranes blocked with iron cations in H_2O buffer; (IIb) PSII(−Mn) membranes blocked with iron cations in D_2O buffer (see the procedure in Materials and Methods). The concentration of the membranes in the EPR tubes was 3.5 mg of Chl/mL, the number of EPR scans was 30, spectra of the samples were measured at 77 K, and the dark samples were dark-adapted at 293 K.

(Figure 10). We conclude that the EPR data show that the different temperature dependences of the Y_Z oxidation and $Y_Z^\bullet$ reduction processes in intact PSII and PSII(−Mn) membranes may be due to different types of hydrogen bonds formed between Y_Z and base B.

We will now discuss physically how a weak hydrogen bond between Y_Z and base B might be converted to a LBHB. In apo-PSII, there is significant solvent access to the Y_Z site, since several exchangeable protons are found in the close vicinity of Y_Z in metal-depleted samples (*10*, *12*, *62*). Rapid, diffusion-controlled oxidation of exogenous donors by the $Y_Z^\bullet$ radical in PSII(−Mn) membranes also indicates direct access of $Y_Z^\bullet$ to solvent (*63*−*65*). In contrast, $Y_Z^\bullet$ is protected by the Mn cluster in intact PSII membranes (*66*), and it is inaccessible to any Mn(II) present in solution (*67*). The microenvironment of Y_Z in the intact system is thought to be "dry" and hydrophobic, whereas that of Y_Z in Mn-depleted samples is "wet" and hydrophilic (*44*). As a consequence, increased solvent access to $Y_Z^\bullet$ due to the loss of the Mn cluster results in the large increase in solvent reorganization energy (λ) from 0.5 eV in intact PSII complexes to 1.6 eV in apo-PSII (*17*, *44*).

Iron binding to the Mn-binding site(s) in Mn-depleted samples prevents exogenous, hydrophilic electron donors [like Mn(II) and Fe(II)] from interacting with $Y_Z^\bullet$ (*37*). Since only solvent (water) access provides such diffusion-controlled migration of exogenous reductants to $Y_Z^\bullet$ (*63*−*65*), Fe binding must lead to structural modification of the environment around Y_Z, which in turn removes water molecules from the area near Y_Z. Moreover, the E_a decrease of the slow component of $Y_Z^\bullet$ reduction in PSII(−Mn), resulting from Fe-blocking the membranes, indicates a decrease in λ, linked with E_a by the following equation (*17*, *44*):

$$E_a = \frac{(G^\circ + \lambda)^2}{4\lambda} - 1/2RT$$

Since the reorganization energy decreases strongly with decreasing water content in the vicinity of the active site (*17*, *44*, *68*), this result also demonstrates a decrease in solvent content around Y_Z in PSII(−Mn, +Fe) samples compared to PSII(−Mn) membranes. The transformation of the environment around Y_Z from a "wet" to a "dry" state should also lead to the lowering of the dielectric constant (ϵ) of the milieu in the vicinity of Y_Z (ϵ of water = 80) to the order of 8−10 as has been suggested for the hydrophobic milieu at P680 site (*69*).

The "squeezing out" of water molecules close to Y_Z, induced by Fe binding to Mn-binding site(s), can be due to the compression of the protein structure around Y_Z. Condensation of protein should also facilitate closer contact between Y_Z and base B, which is consistent with the criteria for the formation of a strong LBHB (*70*). Moreover, creation of a nonpolar milieu in the vicinity of an active center (i.e., Y_Z) can also fulfill a criterion for transformation of a normal weak hydrogen bond to a LBHB, including the matching of the pK_{app} of the proton donor and its acceptor (*54*, *55*, *70*−*72*). As has been suggested, "pK_a" may not be the appropriate terminology to use in a medium shielded from bulk solvent (*72*).

In summary, we have investigated $Y_Z^\bullet$ reduction in the recombination process observed in PSII(−Mn) membranes and the role of the hydrogen bond between Y_Z and base B in this process. Previous results (*10*, *16*, *17*, *21*−*23*) show that this same hydrogen bond also participates in the oxidation of Y_Z. Therefore, we suggest that the hydrogen bond, which is transformed into a LBHB by iron ions, also participates in the oxidation of Y_Z in PSII(−Mn) membranes. Moreover, the interaction of either Mn(II) or Fe(II) ions with the HA_Z Mn-binding site of PSII(−Mn) membranes exhibits quite similar properties, including concentration and pH dependence as well as cation effects (*36*−*38*), and iron ions can restore some properties characteristic of intact PSII membranes incorporating the tetrameric Mn cluster (*23*, *37*). Therefore, the results reported in this paper suggest that in intact PSII membranes the phenolic group of Y_Z also forms an LBHB with base B as has been hypothesized by Zhang & Styring (*32*).

ACKNOWLEDGMENT

The authors thank Dr. Maria L. Ghirardi for many useful discussions as well as her critical reading of the manuscript. B.K.S. appreciates support from Division of Energy Biosciences, Office of Science, U.S. Department of Energy while at NREL and from the Russian Foundation for Basic Research while in Moscow.

APPENDIX

The EPR spectra in Figure 10 were used to calculate the light-minus-dark difference spectra shown in Figure 9. The

light spectra are EPR spectra measured at 77 K from samples frozen under saturating light as described in Materials and Methods. These spectra are a superposition of the EPR spectra of the $Y_Z^\bullet$, $Y_D^\bullet$, and $Chl_Z^\bullet$ light-induced radicals. The dark spectra are EPR spectra of the same samples warmed to 293 K and incubated at this temperature for 2 min in dark. The $Y_Z^\bullet$ and $Chl_Z^\bullet$ radicals are short-lived and disappear rapidly during the dark incubation period, whereas $Y_D^\bullet$ is much more stable (see the discussion in the text related to Figure 7). Therefore, the light-minus-dark EPR difference spectra calculated in Figure 9 represent only $Y_Z^\bullet$.

REFERENCES

1. Diner, B. A. (2001) Amino acid residues involved in the coordination and assembly of the manganese cluster of photosystem II. Proton-coupled electron transport of the redox-active tyrosines and its relationship to water oxidation, *Biochim. Biophys. Acta 1503*, 147−163.
2. Candeias, L. P., Turconi, S., and Nugent, J. H. A. (1998) Tyrosine Y_Z and Y_D of photosystem II: Comparison of optical spectra to those of tyrosine oxidised by pulsed radiolysis, *Biochim. Biophys. Acta 1363*, 1−5.
3. Haumann, M., Mulkijanian, A., and Junge, W. (1999) Tyrosine-Z in oxygen-evolving photosystem II: a hydrogen-bonded tyrosinate, *Biochemistry 38*, 1258−1267.
4. Noguchi, T., Inoue, Y., and Tang, X.-S. (1997) Structural coupling between the oxygen-evolving Mn cluster and a tyrosine residue in photosystem II as revealed by Fourier transform infrared spectroscopy, *Biochemistry 36*, 14705−14711.
5. Rappaport, F., and Lavergne, J. (2001) Coupling of electron and proton transfer in the photosynthetic water oxidase, *Biochim. Biophys. Acta 1503*, 246−259.
6. Hoganson, C. W., and Babcock, G. T. (1988) Electron-transfer events near the reaction center in O_2-evolving photosystem II preparations, *Biochemistry 27*, 5848−5855.
7. Babcock, G. T., Barry, B. A., Debus, R. J., Hoganson, C. W., Atamian, M., McIntosh, L., Sithole, U., and Yocum, C. F. (1989) Water oxidation in photosystem II: from radical chemistry to multielectron chemistry, *Biochemistry 28*, 9557−9565.
8. Barry, B. A., and Babcock, G. T. (1987) Tyrosine radicals are involved in the photosynthetic oxygen-evolving system, *Proc. Natl. Acad. Sci., U.S.A. 84*, 7099−7103.
9. Berthomieu, C., Hienerwadel, R., Boussac, A., Breton, J., and Diner, B. A. (1998) Hydrogen bonding of redox-active tyrosine Z of photosystem II probed by FTIR difference spectroscopy, *Biochemistry* 37, 10547−10554.
10. Diner, B. A., Force, D. A., Randall, D. W., and Britt, R. D. (1998) Hydrogen bonding, solvent exchange, and coupled proton and electron transfer in the oxidation and reduction of redox-active tyrosine Y_Z in Mn-depleted core complexes of photosystem II, *Biochemistry 37*, 17931−17943.
11. Tommos, C., Tang, X.-S., Warncke, K., Hoganson, C. W., Styring, S., McCracken, J., Diner, B. A., and Babcock, G. T. (1995) Spin-density distribution, conformation, and hydrogen bonding of the redox-active tyrosine Y_Z in photosystem II from multiple-electron magnetic-resonance spectroscopies: implications for photosynthetic oxygen evolution, *J. Am. Chem. Soc. 117*, 10325−10335.
12. Tang, X.-S., Zheng, M., Chisholm, D. A., Dismukes, G. C., and Diner, B. A. (1996) Investigation of the differences in the local protein environments surrounding tyrosine radicals $Y_Z^\bullet$ and $Y_D^\bullet$ in photosystem II using wild-type and the D2-Tyr160Phe mutant of *Synechocystis 6803*, *Biochemistry 35*, 1475−1484.
13. Force, D. A., Randall, D. W., Britt, R. D., Tang, X.-S., and Diner, B. A., (1995) 2H ESE-ENDOR study of hydrogen bonding to the tyrosine radicals $Y_D^\bullet$ and $Y_Z^\bullet$ of photosystem II, *J. Am. Chem. Soc. 117*, 12643−12644.
14. Eckert, H.-J., and Renger, G. (1988) Temperature dependence of $P680^+$ reduction in O_2-evolving PSII membrane fragments at different redox states S_i of the water oxidizing system, *FEBS Lett. 236*, 425−431.
15. Ahlbrink, R., Haumann, M., Cherepanov, D., Bögershausen, O., Mulkidjanian, A., and Junge, W. (1998) Function of tyrosin Z in water oxidation by photosystem II: electrostatical promotor instead of hydrogen abstractor, *Biochemistry 37*, 1131−1142.
16. Debus, R. J. (2001) Amino acid residues that modulate the properties of tyrosine Y_Z and the manganese cluster in the water oxidizing complex of photosystem II, *Biochim. Biophys. Acta 1503*, 164−186.
17. Thommos, C., and Babcock, G. T. (2000) Proton and hydrogen currents in photosynthetic water oxidation, *Biochim. Biophys. Acta 1458*, 199−219.
18. Un, S., Tang, X.-S., and Diner, B. A. (1996) 245 GHz high-field EPR study of tyrosine-D zero and tyrosine-Z zero in mutants of photosystem II, *Biochemistry 35*, 679−684.
19. Hays, A.-M. A., Vassiliev, I. R., Golbeck, J. H., and Debus, R. J. (1999) Role of D1-His190 in the proton-coupled oxidation of tyrosine Y_Z in manganese-depleted photosystem II, *Biochemistry 38*, 11851−11865.
20. Conjeaud, H., and Mathis, P. (1980) The effect of pH on the reduction kinetics of *P*-680 in tris-treated chloroplasts, *Biochim. Biophys. Acta 590*, 353−359.
21. Rappaport, F., and Lavergne, J. (1997) Charge recombination and proton transfer in manganese-depleted photosystem II, *Biochemistry 36*, 15294−15302.
22. Mamedov, F., Sayre, R. T., and Sryring, S. (1998) Involvement of histidine 190 on the D1 protein in electron/proton-transfer reactions on the donor side of photosystem II, *Biochemistry 37*, 14245−14256.
23. Semin, B. K., and Seibert, M. (2004) Iron bound to the high-affinity Mn-binding site of the oxygen-evolving complex shifts the p*K* of a component controlling electron transport via Y(Z), *Biochemistry 43*, 6772−6782.
24. Kühne, H., and Brudvig, G. W. (2002) Proton-coupled electron-transfer involving tyrosine Z in photosystem II, *J. Phys. Chem. B 106*, 8189−8196.
25. Roffey, R. A., Kramer, D. M., Govindjee, and Sayre, R. T. (1994)-Lumenal side histidine mutations in the D1 protein of photosystem II affect donor side electron transfer in *Chlamydomonas reinhardtii*, *Biochim. Biophys. Acta 1185*, 257−270.
26. Chu, H.-A., Nguyen, A. P., and Debus, R. J. (1995) Amino acid residues that influence the binding of manganese or calcium to photosystem II. 1. The lumenal interhelical domains of the D1 polypeptide, *Biochemistry 34*, 5839−5858.
27. Hays, A.-M. A., Vassiliev, I. R., Golbeck, J. H., and Debus, R. J. (1998) Role of D1-His190 in proton-coupled electron-transfer reactions in photosystem II: a chemical complementation study, *Biochemistry 37*, 11352−11365.
28. Szalai, V. A., Kühne, H., Lakshmi, K. V., and Brudvig, G. W. (1998) Characterization of the interaction between manganese and tyrosine Z in acetate-inhibited photosystem II, *Biochemistry 37*, 13594−13603.
29. Kodera, Y., Takura, K., Mino, H., and Kawamori, A. (1992) Pulsed EPR study of Tyrosine-Z^+ in photosystem II, In *Research in Photosynthesis*; (Murata, N., Ed.) p 57, Kluwer Academic Publishers Dordrecht, The Netherlands.
30. Shigemori, K., Mino, H., and Kawamori, A. (1997) pH and temperature dependence of tyrosine $Z^\bullet$ decay kinetics in Tris-treated PSII particles studied by time-resolved EPR, *Plant Cell Physiol. 38*, 1007−1011.
31. Nugent, J. H. A., Muhiuddin, I. P., and Evans M. C. W. (2002) Electron transfer from the water oxidizing complex at cryogenic temperatures: the S1 to S2 step, *Biochemistry 41*, 4117−4126.
32. Zhang, C., and Styring, S. (2003) Formation of split electron paramagnetic resonance signals in photosystem II suggests that tyrosine(Z) can be photooxidized at 5 K in the S0 and S1 states of the oxygen-evolving complex, *Biochemistry 42*, 8066−8076.
33. Tamura, N., and Cheniae, G. M. (1987) Photoactivation of the water-oxidizing complex in photosystem II membranes depleted by Mn and extrinsic proteins. I. Biochemical and kinetic characteristics, *Biochim. Biophys. Acta 890*, 179−194.
34. Ananyev, G. M., and Dismukes, G. C. (1996) Assembly of the tetra-Mn site of photosynthetic water oxidation by photoactivation: Mn stoichiometry and detection of a new intermediate, *Biochemistry 35*, 4102−4109.
35. Ono, T., and Inoue, Y. (1984) Ca^{2+}-dependent restoration of O_2-evolving activity in $CaCl_2$ washed PSII particles depleted of 33, 24 and 16 kDa proteins, *FEBS Lett. 168*, 281−286.
36. Semin, B. K., Ivanov, I. I., Rubin, A. B., and Parak, F. (1995) High-specific binding of Fe(II) at the Mn-binding site in Mn-depleted PSII membranes from spinach, *FEBS Lett. 375*, 223−226.
37. Semin, B. K., Ghirardi, M. L., and Seibert, M. (2002) Blocking of electron donation by Mn(II) to $Y_Z^\bullet$ following incubation of

Mn-depleted photosystem II membranes with Fe(II) in the light, *Biochemistry 41*, 5854−5864.
38. Semin, B. K., Davletschina, L. N., Ivanov, I. I., Reiner, M., and Parak, F. (1998) Formation of dinuclear Fe(III) center by interaction of Fe (II) with the Mn-binding site of Mn-depleted PSII membranes, in *Photosynthesis: Mechanisms and Effects* (Garab, G., Ed.) Vol. 2, pp 1415−1418, Kluwer Academic Publishers, Dordrecht, The Netherlands.
39. Porra, R. J., Tompson, W. A., and Kriedemann, P. E. (1989) Determination of accurate extinction coefficients and simultaneous-equations for assaying chlorophyll-A and chlorophyll-B extracted with 4 different solvents − verification of the concentration of chlorophyll standards by atomic-absorption spectroscopy, *Biochim. Biophys. Acta 975*, 384−394.
40. Preston, C., and Seibert, M. (1991) Protease treatments of photosystem II membrane fragments reveal that there are four separate high-affinity Mn-binding sites, *Biochemistry 30*, 9625−9633.
41. Schowen, R. L. (1977) Solvent isotope effects on enzymic reactions, in *Isotope Effect on* Enzyme-Catalyzed Reactions (Cleland, W. W., O'Leary, M. H., Northrop, D. B., Eds.), pp 64−99, University Park Press, Baltimore, MD.
42. Ghirardi, M. L., Lutton, T. W., and Seibert, M. (1996) Interactions between diphenylcarbazide, zinc, cobalt, and manganese on the oxidizing side of photosystem II, *Biochemistry 35*, 1820−1828.
43. Reinman, S., and Mathis, P. (1981) Influence of temperature on photosystem II electron-transfer reactions, *Biochim. Biophys. Acta 635*, 249−258.
44. Renger, G., Christen, G., Karge, M., Eckert, H.-J., and Irrgang, K.-D. (1998) Application of the Marcus theory for analysis of the temperature dependence of the reactions leading to photosynthetic water oxidation: results and implications, *J. Biol. Inorg. Chem. 3*, 360−366.
45. Nixon, P. J., and Diner, B. A. (1992) Aspartate 170 of the photosystem II reaction center polypeptide D1 is involved in the assembly of the oxygen-evolving manganese cluster, *Biochemistry 31*, 942−948.
46. Ono, T.-A., and Mino, H. (1999) Unique binding site for Mn^{2+} ion responsible for reducing an oxidized Y_Z tyrosine in manganese-depleted photosystem II membranes, *Biochemistry 38*, 8778−8785.
47. Joliot, A., and Joliot, P. (1964) Kinetic study of the photochemical reaction liberating oxygen during photosynthesis, *C. R. Acad. Sci. Paris 258*, 4622−4625.
48. Melis, A., and Homann, P. H. (1978) A selective effect of Mg^{2+} on the photochemistry of one type of reaction center in photosystem 2 of chloroplasts, *Arch. Biochim. Biophys. 190*, 523−530.
49. Segel, I. H. (1993) *Enzyme Kinetics: Behavior and Analysis of Rapid Equilibrium and Steady-State Enzyme Systems*, Wiley-Interscience, New York.
50. Jeans, C., M. J. Schilstra, M. J., and D. R. Klug, D. R. (2002) The temperature dependence of P680(+) reduction in oxygen-evolving photosystem II, *Biochemistry 41*, 5015−5023.
51. Christen, G., Seeliger, A. G., and Renger, G. (1999) P680(+)* reduction kinetics and redox transition probability of the water oxidizing complex as a function of pH and H/D isotope exchange in spinach thylakoids, *Biochemistry 38*, 6082−6092.
52. Vrettos, J. S., Limburg, J., and Brudvig, G. W. (2001) Mechanism of photosynthetic water oxidation: combining biophysical studies of photosystem II with inorganic model chemistry, *Biochim. Biophys. Acta 1503*, 229−245.
53. Perrin, C. L., and Nielson, J. B. (1997) "Strong" hydrogen bonds in chemistry and biology, *Annu. Rev. Phys. Chem. 48*, 511−544.
54. Cleland, W. W., Frey, P. A., and Gerlt, J. A. (1998) The low barrier hydrogen bond in enzymatic catalysis, *J. Biol. Chem. 273*, 25529−25532.
55. Mildvan, A. S., Harris, T. K., and Abeygunawardana, C. (1999) Nuclear magnetic resonance methods for the detection and study of low-barrier hydrogen bonds on enzymes, *Methods Enzymol. 308*, 219−245.
56. Hibbert, F., and Emsley, J. (1990) Hydrogen bonding and chemical reactivity, *Adv. Phys. Org. Chem. 26*, 255−380.
57. Mildvan, A. S., Massiah, M. A., Harris, T. K., Marks, G. T., Harrison, D. H. T., Viragh, C., Reddy, P. M., and Kovach, I. M. (2002) Short, strong hydrogen bonds on enzymes: NMR and mechanistic studies, *J. Mol. Struct. 615*, 163−175.
58. Karge, M., Irrgang, K.-D., Sellin, S., Feinaugle, R., Liu, B., Eckert, H.-J., Eichler, H. J., and Renger, G. (1996) Effects of hydrogen/deuterium exchange on photosynthetic water cleavage in PS II core complexes from spinach, *FEBS Lett. 378*, 140−144.
59. Cowin, J. P., Tsekouras, A. A., Iedema, M. J., Wu, K., and Ellison, G. B. (1999) Immobility of protons in ice from 30 to 190 K, *Nature 398*, 405−407.
60. Tracewell, C. A., Vrettos, J. S., Bautista, J. A., Frank, H. A., and Brudvig, G. W. (2001) Carotenoid photooxidation in photosystem II. *Arch. Biochem. Biophys. 385*, 61−69.
61. Pujols-Ayala, I., and Barry, B. A. (2002) Histidine 190-D1 and Glutamate 189-D1 provide structural stabilization in photosystem II, *Biochemistry 41*, 11456−11465.
62. Tommos, C., McCracken, J., Styring, S., and Babcock, G. T. (1998) Stepwise Disintegration of the Photosynthetic Oxygen-Evolving Complex *J. Am. Chem. Soc. 120*, 10441−10452.
63. Babcock, G. T., and Sauer, K. (1975) Two electron donation sites for exogenous reductants in chloroplast photosystem 2, *Biochim. Biophys. Acta 396*, 48−62.
64. Ghanotakis, D. F., Yerkes, C. T., and Babcock, G. T. (1982) The role of reagents accelerating the deactivation reactions of water-splitting enzyme system Y (ADRY reagents) in destabilizing high-potential oxidizing equivalents generated in chloroplast photosystem, *Biochim. Biophys. Acta 682*, 21−31.
65. Babcock, G. T., Ghanotakis, D. F., Ke, B., and Diner, B. A. (1983) Electron donation to photosystem II in reaction center preparations, *Biochim. Biophys. Acta 723*, 276−286.
66. Ghanotakis, D. F., Babckock, G. T., and Yocum, C. F. (1984) Structural and catalytic properties of the oxygen-evolving complex. Correlation of polypeptide and manganese release with the behavior of Z^+ in chloroplasts and a highly resolved preparation of the PSII complex, *Biochim. Biophys. Acta 765*, 388−398.
67. Chroni, S., and Ghanotakis, D. F. (2001) Accessibility of tyrosine Y_Z to exogenous reductants and Mn^{2+} in various photosystem II preparations, *Biochim. Biophys. Acta 1504*, 432−437.
68. Mertz, E. L., and Krishtalik, L. I. (2000) Low dielectric response in enzyme active site, *Proc. Natl. Acad. Sci., USA 97*, 2081−2086.
69. Mulkidjanian, A. Y. (1999) Photosystem II of green plants: on the possible role of retarded protonic relaxation in water oxidation, *Biochim. Biophys. Acta 1410*, 1−6.
70. Frey, P. A., Whitt, S. A., and Tobin, J. B. (1994) A low-barrier hydrogen bond in the catalytic triad of serine proteases, *Science 264*, 1927−1930.
71. Gerlt, J. A., and Gassman, P. J. (1992) Understanding enzyme-catalized proton abstraction from carbon acids: details of stepwise mechanisms for β-elimination reactions, *J. Am. Chem. Soc. 114*, 5928−5934.
72. Ha, N.-C., Kim, M.-S., Lee, W., Choi, K. Y., and Oh, B.-H. (2000) Detection of large pK_a perturbations of an inhibitor and a catalytic group at an enzyme active site, a mechanistic basis for catalytic power of many enzymes, *J. Biol. Chem. 275*, 41100−41106.

BI047618W